



This information is current as  
of August 1, 2025.

## **Multisite Benchmark Study for Standardized Relative CBV in Untreated Brain Metastases Using the DSC-MRI Consensus Acquisition Protocol**

Sarah Kohn Loizzo, Melissa A. Prah, Min J. Kong, Daniel Phung, Javier C. Urcuyo, Jason Ye, Frank J. Attenello, Jesse Mendoza, Yuxiang Zhou, Mark S. Shiroishi, Leland S. Hu and Kathleen M. Schmainda

*AJNR Am J Neuroradiol* 2025, 46 (3) 529-535

doi: <https://doi.org/10.3174/ajnr.A8531>

<http://www.ajnr.org/content/46/3/529>

# Multisite Benchmark Study for Standardized Relative CBV in Untreated Brain Metastases Using the DSC-MRI Consensus Acquisition Protocol

Sarah Kohn Loizzo,  Melissa A. Prah,  Min J. Kong,  Daniel Phung, Javier C. Urcuyo, Jason Ye, Frank J. Attenello, Jesse Mendoza,  Yuxiang Zhou,  Mark S. Shiroishi,  Leland S. Hu, and  Kathleen M. Schmainda



## ABSTRACT

**BACKGROUND AND PURPOSE:** A national consensus recommendation for the collection of DSC-MRI perfusion data, used to create maps of relative CBV (rCBV), has been recently established for primary and metastatic brain tumors. The goal was to reduce inter-site variability and improve ease of comparison across time and sites, fostering widespread use of this informative measure. To translate this goal into practice, the prospective collection of consensus DSC-MRI data and characterization of derived rCBV maps in brain metastases is needed. The purpose of this multisite study was to determine rCBV in untreated brain metastases in comparison to glioblastoma (GBM) and normal-appearing brain by using the national consensus protocol.

**MATERIALS AND METHODS:** Subjects from 3 sites with untreated enhancing brain metastases underwent DSC-MRI according to a recommended option that uses a midrange flip angle, GRE-EPI acquisition, and the administration of both a preload and second DSC-MRI dose of 0.1 mmol/kg gadolinium-based contrast agent. Quantitative maps of standardized relative CBV (srCBV) were generated and enhancing lesion ROIs determined from postcontrast T1-weighted images alone or calibrated difference maps, termed  $\Delta$  T1 (dT1) maps. Mean srCBV for metastases were compared with normal-appearing white matter (NAWM) and GBM from a previous study. Comparisons were performed by using either the Wilcoxon signed-rank test for paired comparisons or the Mann-Whitney *U* nonparametric test for unpaired comparisons.

**RESULTS:** Forty-nine patients with a primary histology of lung ( $n = 25$ ), breast ( $n = 6$ ), squamous cell carcinoma ( $n = 1$ ), melanoma ( $n = 5$ ), gastrointestinal (GI) ( $n = 3$ ), and genitourinary (GU) ( $n = 9$ ) were included in comparison to GBM ( $n = 31$ ). The mean srCBV of all metastases ( $1.83 \pm 1.05$ ) were significantly lower ( $P = .0009$ ) than mean srCBV for GBM ( $2.67 \pm 1.34$ ) with both statistically greater ( $P < .0001$ ) than NAWM ( $0.68 \pm 0.18$ ). Histologically distinct metastases are each statistically greater than NAWM ( $P < .0001$ ) with lung ( $P = .0002$ ) and GU ( $P = .02$ ) srCBV being significantly different from GBM srCBV.

**CONCLUSIONS:** Using the consensus DSC-MRI protocol, mean srCBV values were determined for treatment-naïve brain metastases in comparison to normal-appearing white matter and GBM thus setting the benchmark for all subsequent studies adherent to the national consensus recommendation.

**ABBREVIATIONS:** BSW = Boxerman Schmainda Weisskoff; dT1 =  $\Delta$  T1; GBCA = gadolinium-based contrast agent; GBM = glioblastoma; GI = gastrointestinal; GRE = gradient echo; GU = genitourinary; NAWM = normal-appearing white matter; nCBV = normalized relative CBV; PSR = percent signal recovery; rCBV = relative CBV; SCC = squamous cell carcinoma; srCBV = standardized relative CBV; TIW = T1-weighted

Brain metastasis is the most common tumor of the central nervous system, and the incidence is on the rise. One estimate reports the annual number of identified cases in the United States

to be 23,598.<sup>1</sup> Yet, additional clinical data suggest that more than 100,000 patients develop brain metastases each year.<sup>2</sup> This substantial and increasing disease burden is in part due to an overall increase of primary cancers, but also better systemic therapies that increase the probability of metastatic disease as the patients live longer.<sup>3</sup> The most common primary cancers are lung cancer, breast cancer, and melanoma occurring in approximately 40%–50%, 15%–20%, and 5%–20% of patients newly diagnosed with

Received April 26, 2024; accepted after revision August 27.

From the Department of Radiation Oncology (S.K.L.) and Biophysics (M.A.P., K.M.S.), Medical College of Wisconsin, Milwaukee, Wisconsin; Departments of Radiology (M.J.K., Y.Z., L.S.H.), Cancer Biology (L.S.H.), and Neurological Surgery (L.S.H.), and Mathematical Neuro-Oncology Lab (J.C.U.), Mayo Clinic Arizona, Phoenix, Arizona; Departments of Radiology (D.P., J.M., M.S.S.), Radiation Oncology (J.Y.), Neurological Surgery (F.J.A.), and Population and Public Health Sciences (M.S.S.), Keck School of Medicine of the University of Southern California, Los Angeles, California; and Imaging Genetics Center (M.S.S.), USC Mark and Mary Stevens Neuroimaging and Informatics Institute, Marina del Rey, California.

Mark S. Shiroishi, Leland S. Hu, and Kathleen M. Schmainda contributed equally to this article.

Please address correspondence to Kathleen M. Schmainda, PhD, Department of Biophysics, Medical College of Wisconsin, 8701 Watertown Plank Rd, Milwaukee, WI 53226; e-mail: kathleen@mcw.edu

<http://dx.doi.org/10.3174/ajnr.A8531>

## SUMMARY

**PREVIOUS LITERATURE:** The importance of obtaining perfusion-weighted MRI data, most commonly DSC-MRI data, is being increasingly recognized for the evaluation of brain metastasis. However, a lack of consistency in brain tumor perfusion studies, attributable to a lack of standard protocol, has resulted in a wide range of relative CBV values that are inconsistent and difficult to reproduce between studies. To overcome this limitation a consensus protocol has been developed and used for the current studies in treatment-naïve brain metastases.

**KEY FINDINGS:** First steps toward establishing consensus-acquisition benchmark values for srCBV in brain metastases has been accomplished. The srCBV can be used to distinguish brain metastases from normal-appearing brain and are generally less than srCBV for glioblastoma.

**KNOWLEDGE ADVANCEMENT:** The results of this study should enable greater consistency and cross-site comparisons of srCBV for the evaluation of both treated and untreated brain metastases.

brain metastases.<sup>4</sup> The average survival for patients with brain metastases is less than 6 months.<sup>2</sup>

Standard anatomic MRI, obtained with the administration of a gadolinium-based contrast agent (GBCA), is central to the diagnosis of brain metastases.<sup>3</sup> Yet, the importance of also obtaining perfusion-weighted MRI data, most commonly DSC-MRI data, is being increasingly recognized. DSC-MRI, from which maps of relative CBV (rCBV) can be generated, help to differentiate brain metastases from normal brain tissue and potentially distinguish brain metastases from primary brain tumors.<sup>5</sup> The use of rCBV has also been encouraged for distinguishing progressive tumor from pseudoprogression often due to posttreatment radiation effects,<sup>3</sup> which often appear similar on postcontrast MRI.<sup>6</sup>

However, a lack of consistency in brain tumor perfusion studies, attributable to a lack of standard protocol, has resulted in a wide range of rCBV values that are inconsistent and difficult to reproduce between studies.<sup>6</sup> Likewise, as summarized in Fig 1, a wide range of MRI settings have been used for DSC-MRI studies in metastatic brain tumors,<sup>7–29</sup> all of which affect the quality and accuracy of derived rCBV maps.<sup>30</sup> This variability may limit the ability of rCBV to identify metastases in distinction from normal brain and/or differentiate metastases from glioblastoma (GBM), for example. Pretreatment differentiation of these 2 most common intra-axial brain tumors is essential given the substantial difference in clinical work-up and treatment strategies for each.<sup>31</sup> Consequently, while most studies suggest that the mean rCBV in brain metastases is less than GBM given their well-characterized high vascularity,<sup>32</sup> it is not surprising that the margin of difference ranges from negligible to statistically significant. In response, a multi-investigator, multi-institutional working group was convened to formulate a national consensus recommendation for DSC-MRI data acquisition and postprocessing.<sup>33</sup> This recommendation, initially developed for primary brain tumors, was also adopted for DSC-MRI of brain metastases.<sup>3</sup> Still, as Fig 1 confirms, this also means that benchmark rCBV values, determined with the consensus protocol, are lacking. It was therefore the goal of this study to establish rCBV benchmark values for metastatic brain tumors beginning with treatment-naïve brain metastases. We hypothesize that the determination of benchmark rCBV values will enable the generalization of results that address questions of whether rCBV can be used to distinguish brain

metastases from normal-appearing brain, or primary brain tumor and/or in distinction from metastases of different primary histology. To begin to address this goal, we chose to compute standardized relative CBV (srCBV)<sup>34</sup> as opposed to normalized relative CBV (nrCBV), the latter of which requires the subjective determination of a normalizing reference ROI. For srCBV, a predetermined calibration is used to generate quantitative srCBV maps precluding the need for a reference ROI. Consequently, srCBV provides more repeatable and consistent results across time and patients,<sup>35,36</sup> increasing the likelihood of distinguishing tissue types with threshold values that can be widely applied.

## MATERIALS AND METHODS

### Patients

All participants were enrolled in this Health Insurance Portability and Accountability Act-compliant study according to the institutional review board policy and approvals at each of 3 participating institutions (Medical College of Wisconsin, Mayo Clinic-Arizona, Keck School of Medicine of University of Southern California). Patients considered for inclusion were those with treatment-naïve brain metastases who underwent an MRI examination that included DSC-MRI perfusion imaging. All diagnoses for metastases were confirmed surgically after biopsy or resection. Also included for comparison were participants from a single institution (Medical College of Wisconsin) who had histologically confirmed treatment-naïve high-grade glioma with preoperative DSC-MRI.<sup>37</sup>

### Imaging

All MRI examinations were performed on 3T MRI systems. Standard precontrast FLAIR and T1-weighted (T1W) spin-echo imaging were obtained according to the clinical protocol at each site with postcontrast T1W images obtained after administration of a 0.1 mmol/kg dose of a GBCA. The pre- and postcontrast T1W images used the same acquisition parameters so that calibrated difference maps, referred to as  $\Delta$  T1 (dT1) maps, could be determined as previously described.<sup>38</sup> One of the 2 recommended consensus protocol options was used for all patients.<sup>3,33</sup> For this option the first GBCA dose (0.1 mmol/kg) serves as a preload for the subsequent DSC-MRI data collection. Then, a second GBCA dose (0.1 mmol/kg) is administered at 40–60 seconds during the acquisition of GRE-EPI (FOV = 220 mm, matrix = 96 × 96 or

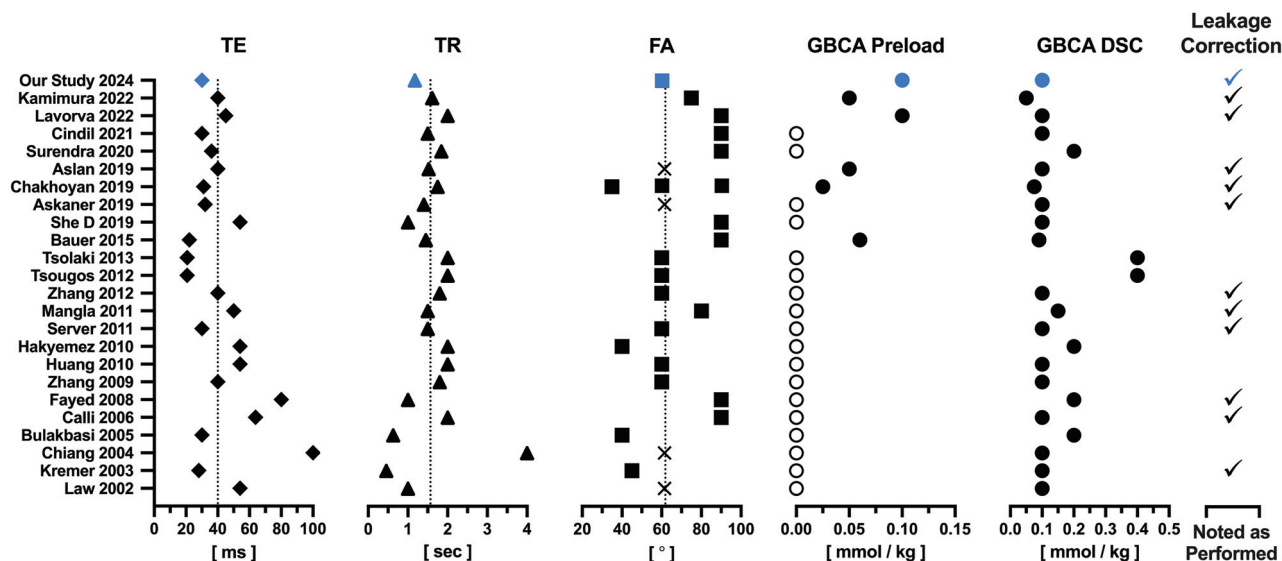


**FIG 1.** Summary of DSC-MRI parameter settings for studies that reported rCBV values for brain metastases. The studies were identified by performing a literature search by using PubMed and Ovid Medline. The PubMed selection criteria used were “brain neoplasm\*” OR “brain neoplasms” [MESH] OR “neoplasm metasta\*” OR “brain metasta\*” AND (“rCBV” or “relative cerebral blood”) AND (“DSCMRI” OR “DSC MRI” OR (“dynamic susceptibility contrast” AND (“MR” OR “Magnetic Resonance Imaging” [MESH] OR “MRI”))), which yielded 248 publications. The Ovid Medline parameters used brain neoplasm, neoplasm metastases, brain metastases yielding 389,714 publications. Further including cerebrovascular circulation or relative CBF, DSCMRI or DSC MRI or dynamic susceptibility yielded 1240 publications. The inclusion of contrast and (MR or MRI) yielded 313 publications. Limited further to English language and humans yielded 212 publications. With both Pubmed and Ovid Medline 23 studies resulted that reported an intratumoral rCBV value of brain metastases.<sup>7–29</sup> For these the DSC-MRI parameter settings are listed above along with the consensus settings used in the current study. Note the wide range in values used. The *dashed line* indicates median settings across all studies for TE, TR, and flip angle. Average values are shown for studies that reported a range of values, where unreported settings are designated with an “X.” *Unfilled circles* indicate studies for which a GBCA preload was not given. Mean values are shown when ranges were given. Settings used for our study are shown in *blue*.

128 × 128, slice thickness = 4–5 mm) by using recommended parameter settings (flip angle = 60°, TE/TR = 30 ms/1100–1250 ms). The GRE-EPI data were collected for a total duration of 120 seconds. When the DSC-MRI slices were not an exact subset of the T1W slices, an additional T1W “reference” scan was obtained by using a slice prescription (orientation and spacing) matching the DSC-MRI examination for ease of coregistering the DSC-MRI to the anatomic images.

**Image and Statistical Analysis.** srCBV values were calculated onsite at each institution. This was made possible with the platform-independent IB Rad Tech plug-in (Imaging Biometrics) available at each site. IB Rad Tech was used with either the Horos (<https://horosproject.org>) or OsiriX (<https://www.osirix-viewer.com>) DICOM viewers. The customizable IB Rad Tech plug-in was designed to guide the user through the desired postprocessing steps, most of which are automatic but allow user oversight. For this study these steps included registration of the T1W and DSC-MRI series, generation of dT1 maps,<sup>38</sup> for delineation of contrast-enhancing ROIs, and creation of srCBV<sup>34</sup> with leakage correction.<sup>39</sup> Specifically, first pre- and postcontrast T1W images are registered and individually standardized.<sup>38</sup> Next, dT1 maps are computed from the difference between the registered and standardized post- and precontrast T1W images. The dT1 facilitate the visualization of the enhancing lesion, free of intrinsically increased T1 signal from, for example, blood products or proteinaceous material. Next, the user is prompted to draw a rough-bounding ROI around the enhancing lesion. Because dT1

maps are quantitative, a single, previously determined threshold is applied and an enhancing tumor ROI is generated.<sup>38</sup> Next, the T1W and DSC-MRI series are registered and leakage-corrected, calibrated srCBV<sup>34</sup> generated.<sup>39</sup> Unlike nrCBV maps, srCBV do not require user-drawn reference ROIs for normalization. Mean srCBV for metastases are determined using the dT1 ROIs (or postcontrast T1W ROIs when dT1 were not available), and compared with srCBV in untreated GBM from a previous study.<sup>37</sup> Mean srCBV, from ROIs drawn within contralateral normal-appearing white matter (NAWM) of each brain metastasis patient, were also determined for purposes of comparison with normal-appearing brain tissue. The srCBV for GBM and each group of metastases for a specific primary cancer were also compared with the NAWM from all metastases, a choice supported by the consistency of NAWM rCBV values when standardized.<sup>34</sup> The Wilcoxon matched-pairs signed rank test was used to compare the metastases and NAWM srCBV data as this is a paired data set. For the remainder of comparisons, the Mann-Whitney *U* nonparametric test was used. For both analyses a *P* < .05 was considered significant.

## RESULTS

Forty-nine patients, from 3 institutions (Medical College of Wisconsin = 28, University of Southern California = 12, Mayo Clinic Arizona = 9), with treatment-naïve brain metastases met inclusion criteria for this study. The preoperative DSC-MRI studies took place between November 21, 2006 and September 21, 2020. The median age was 62 years with a range of 28–78 years.

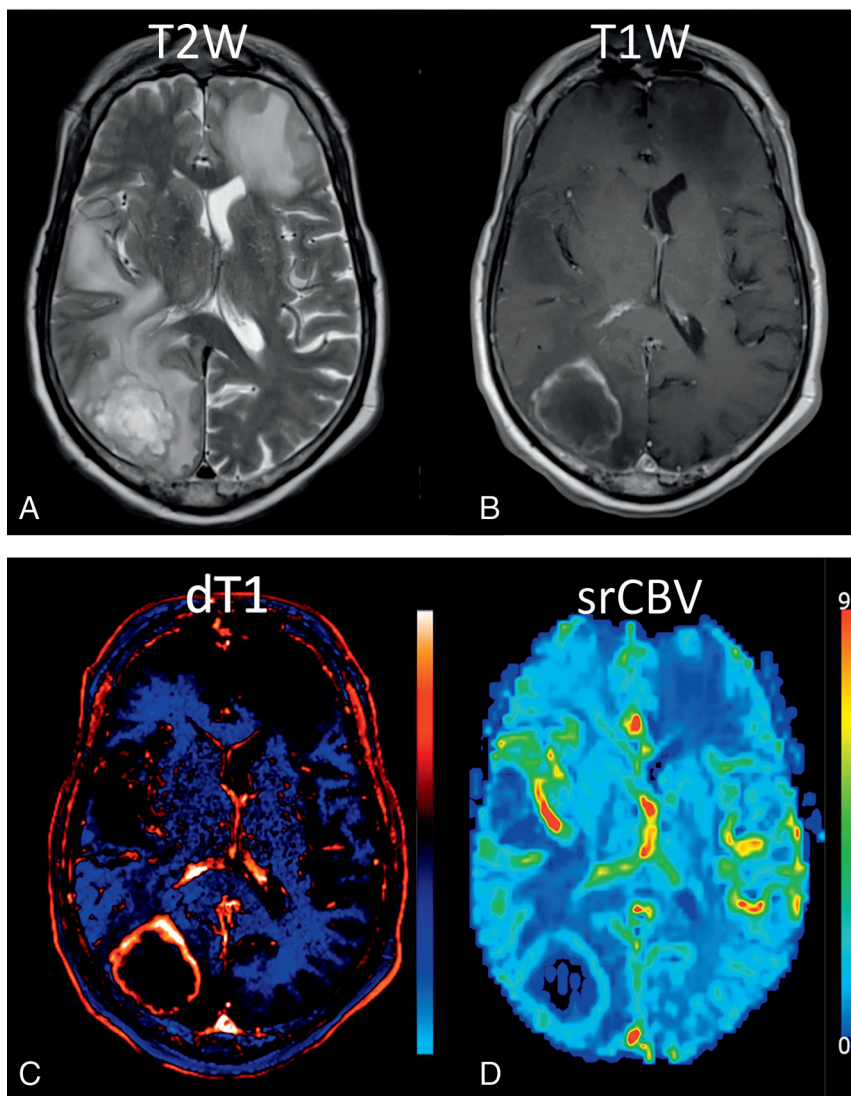


**FIG 2.** MRI study obtained in a 64-year-old male patient with primary lung cancer. Shown are (A) a T2W image, (B) postcontrast T1W image, (C) dT1 map, and (D) corresponding srCBV map of 1 image slice showing the rim-enhancing brain metastasis. The mean srCBV, for all lesions on all image slices, is  $1.56 \pm 1.40$ .

The patients included 23 men and 26 women. The primary histology for the brain metastases included lung ( $n = 25$ ), breast ( $n = 6$ ), squamous cell carcinoma (SCC) ( $n = 1$ ), melanoma ( $n = 5$ ), gastrointestinal (GI) ( $n = 3$ ), and genitourinary (GU) ( $n = 9$ ). An additional 31 patients with histologically confirmed GBM (according to the World Health Organization 2016 classification<sup>40</sup>), who underwent preoperative DSC-MRI from 2010–2014, were included for comparison. The GBM data were included in a previously published report.<sup>37</sup>

An example MRI study with a corresponding srCBV map is shown in Fig 2 for a 64-year-old male patient with primary lung cancer. The mean srCBV for all metastases ( $1.83 \pm 1.05$ ) is significantly lower ( $P = .0009$ ) than the mean srCBV for GBM ( $2.67 \pm 1.34$ ) with both statistically greater ( $P < .0001$ ) than NAWM ( $0.68 \pm 0.18$ ) (Fig 3A). The srCBV for histologically distinct metastases are also shown (Fig 3B) with each being statistically greater than NAWM ( $P < .0001$ ) except for SCC, which is

nonevaluable given  $n = 1$ . Lung ( $P = .0002$ ) and GU ( $P = .02$ ) srCBV were significantly less than GBM srCBV while breast ( $P = .76$ ), melanoma ( $P = .86$ ), and GI ( $P = .41$ ) srCBV were not. The individual srCBV mean and standard deviation are as follows: lung ( $1.54 \pm 0.59$ ), breast ( $2.28 \pm 0.87$ ), melanoma ( $2.48 \pm 1.24$ ), GI ( $1.91 \pm 0.64$ ), and GU ( $2.01 \pm 1.88$ ).

## DISCUSSION

By means of DSC-MRI perfusion imaging, which is consistent with the established consensus protocol for primary brain tumors<sup>33</sup> and incorporated for brain metastases,<sup>3</sup> data obtained from 3 sites demonstrate that brain metastases of different primary origins have srCBV values that in general are significantly greater than NAWM, but significantly lower than srCBV for GBM. Unique to this study, srCBV values of brain metastases were determined by using the consensus DSC-MRI protocol.

The results of this study confirm that srCBV should be helpful in identifying brain metastases as distinct from normal brain. These results reflect the fact that new vessel formation (ie, angiogenesis) is a hallmark of brain metastases development.<sup>41</sup> Yet, given the reported variability in the degree of angiogenesis based on primary histology it was unclear that this result would apply to all metastases. SCC was the only metastatic type not showing this distinction. But, with only 2 patients with SCC, a firm conclusion is not possible for this primary histology and a larger study is warranted.

Similarly, metastatic srCBV was found to be less than GBM srCBV, a finding consistent with the well-known highly angiogenic nature of GBM. However, the results were mixed when comparing individual metastases in comparison with GBM. This is likely due to variations in angiogenesis for different metastatic types, but also to smaller numbers of patients for some categories. Even so, for all cases, metastatic mean srCBV was less than GBM mean srCBV suggesting the possibility of distinction of untreated primary GBM from metastatic tumor types based on srCBV alone. While a recent study demonstrated that percent signal recovery (PSR), determined from the raw DSC signal, was better than rCBV for distinguishing lymphoma and primary and metastatic tumor types<sup>26</sup> these comparisons were performed by using suboptimal DSC-MRI acquisition settings different from the national recommendation and did not include a comparison with standardized rCBV. Therefore, whether srCBV or PSR is best for this distinction remains an open question. Alternatively, it is possible that a

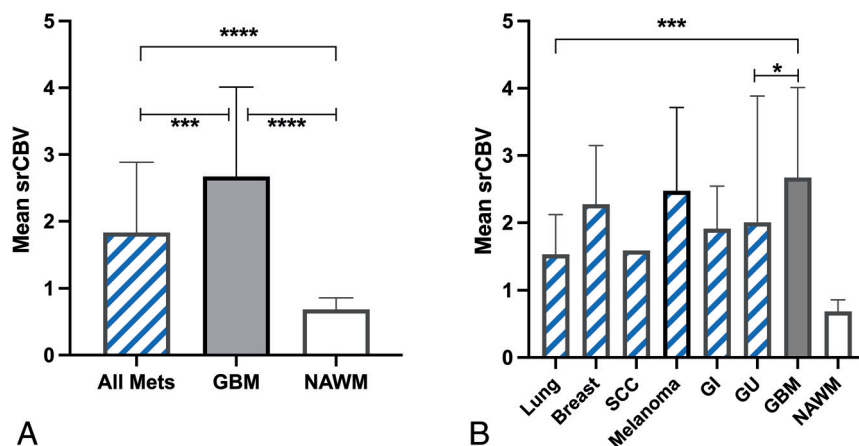


**FIG 3.** Mean srCBV (A) for all metastases ( $1.83 \pm 1.05$ ) is statistically less than that for GBM ( $2.67 \pm 1.34$ ) ( $P = .0009$ ) and significantly greater than the mean srCBV for NAWM ( $0.68 \pm 0.18$ ) ( $P < .0001$ ). Likewise, mean srCBV for GBM is statistically greater than for NAWM ( $P < .0001$ ). B, The srCBV for histologically distinct metastases are each statistically greater than NAWM ( $P < .0001$ ), except for metastatic SCC, which is nonevaluable with  $n = 1$ . Lung ( $P < .0002$ ) and GU ( $P = .02$ ) rCBV are also significantly different from GBM. The individual srCBV mean, standard deviation, and numbers ( $n$ ) for each of histologically distinct brain metastases are lung ( $1.54 \pm 0.59$ ,  $n = 25$ ), breast ( $2.28 \pm 0.87$ ,  $n = 6$ ), SCC ( $1.59$ ,  $n = 1$ ), melanoma ( $2.48 \pm 1.24$ ,  $n = 5$ ), GI ( $1.91 \pm 0.64$ ,  $n = 3$ ), and GU ( $2.01 \pm 1.88$ ,  $n = 9$ ) as compared with GBM ( $2.67 \pm 1.34$ ,  $n = 31$ ) and NAWM ( $0.68 \pm 0.18$ ,  $n = 49$ ).

combination of PSR and srCBV may provide the best distinction of these tumor types.

While all data in this study were collected with 1 of the 2 recommended acquisition options, previous studies have demonstrated the equivalence of these acquisition options for standardized rCBV.<sup>42</sup> Thus, we contend that comparable thresholds would likewise be determined if the single-dose low FA acquisition option were used. In addition to using the consensus recommendation for the acquisition of the perfusion MRI, we also followed the recommendation to incorporate leakage correction as part of the postprocessing.<sup>33</sup> Though a particular leakage correction algorithm was not specified as part of the consensus recommendation, we used one of the most common and well-published/proved approaches, referred to as the BSW (Boxerman, Schmainda, Weisskoff) leakage correction method.<sup>39</sup> As previously demonstrated, if rCBV maps are not corrected for leakage effects, their correlation with tumor aggressiveness is lost.<sup>39,43</sup> In addition, only when BSW leakage correction was applied did the single-dose consensus option give results equivalent to the standard double-dose option.<sup>42</sup>

srCBV rather than nrCBV was used in this study. The rationale is based on studies showing that srCBV, while providing information comparable to nrCBV, is more consistent than nrCBV, with lower coefficient of variation<sup>34</sup> and improved repeatability<sup>35</sup> across time points. This greater consistency is due, at least in part, to the fact that srCBV does not require the manual delineation of a reference ROI, which also makes possible the seamless and routine integration of automatic srCBV map generation into the daily workflow. Furthermore, the fact that the standardization of rCBV results in a quantitative rCBV map has far reaching implications for the determination of thresholds to distinguish tissue and tumor types, which can be broadly applied. A recent example is the srCBV thresholds determined to distinguish high-grade tumor from treatment effect.<sup>44</sup> This threshold is being used for the creation of fractional tumor burden maps<sup>45</sup>

with clinically confirmed benefit to distinguish tumor progression from pseudoprogression.<sup>28,46,47</sup>

Several previous studies have likewise demonstrated that normalized rCBV is increased in primary brain tumors compared with brain metastases and NAWM.<sup>11–13,15,17,21–23,29,48</sup> However, there are large variations across sites, most likely due to differences in both the MRI acquisition protocols and postprocessing methods used (Fig 1), making the data difficult to reproduce. This study uses data collected with the recently published consensus protocol together with one of the mostly widely used approaches for leakage correction thereby establishing a benchmark for all forthcoming studies seeking to use DSC-MRI for the evaluation of brain metastases.

As previously described it was possible for srCBV to be calculated in the

same way at each site by using a customizable software plug-in available at each institution. The processing workflow can be customized according to the needs of each study or site, with respect to order of processing, types and names of input images and types of output parameter maps. Yet the core processing modules to create parameter maps, such as dT1 and srCBV, remain fixed. This flexibility coupled with algorithmic consistency makes possible the widespread adoption and consistency of methodology and reported results across sites.

Study limitations include a small study population, with small numbers of patients in categories with less common metastases. Also, the focus was on untreated brain metastases only. However, the results motivate additional studies with more subjects, which may also help to address the possibility of making further distinctions among metastases resulting from different primary cancers. In addition, knowledge of untreated brain metastases is the first step toward addressing the utility of DSC-MRI for the evaluation of treated metastases. As with primary brain tumors, there is mounting evidence to indicate that rCBV can better distinguish tumor progression from nontumor treated tissue than standard MRI alone.<sup>6,44,49</sup>

## CONCLUSIONS

Using the consensus DSC-MRI acquisition protocol we have confirmed the utility of standardized rCBV to identify biologically active, treatment-naïve brain metastases as distinguished from NAWM and GBM thus setting the benchmark for all subsequent studies adherent to the national consensus recommendation.

## ACKNOWLEDGMENTS

Sincere appreciation to Medical College of Wisconsin research coordinators, Cathy Marszalkowski and Jaimy Pettit.

Disclosure forms provided by the authors are available with the full text and PDF of this article at [www.ajnr.org](http://www.ajnr.org).

## REFERENCES

- Cagney DN, Martin AM, Catalano PJ, et al. Incidence and prognosis of patients with brain metastases at diagnosis of systemic malignancy: a population-based study. *Neuro Oncol* 2017;19:1511–21 [CrossRef Medline](#)
- Stelzer K. Epidemiology and prognosis of brain metastases. *Surg Neurol Int* 2013;4:S192–202 [CrossRef Medline](#)
- Kaufmann TJ, Smits M, Boxerman J, et al. Consensus recommendations for a standardized brain tumor imaging protocol for clinical trials in brain metastases. *Neuro Oncol* 2020;22:757–72 [CrossRef Medline](#)
- Eichler AF, Plotkin SR. Brain Metastases Opinion statement. *Curr Treat Options Neurol* 2008;10:308–14 [CrossRef Medline](#)
- Derks SHAE, van der Veldt AAM, Smits M. Brain metastases: the role of clinical imaging. *Br J Radiology* 2022;95:20210944 [CrossRef Medline](#)
- Patel P, Baradaran H, Delgado D, et al. MR perfusion-weighted imaging in the evaluation of high-grade gliomas after treatment: a systematic review and meta-analysis. *Neuro Oncol* 2017;19:118–27 [CrossRef Medline](#)
- Law M, Cha S, Knopp EA, et al. High-grade gliomas and solitary metastases: differentiation by using perfusion and proton spectroscopic MR imaging. *Radiology* 2002;222:715–21 [CrossRef Medline](#)
- Kremer S, Grand S, Berger F, et al. Dynamic contrast-enhanced MRI: differentiating melanoma and renal carcinoma metastases from high-grade astrocytomas and other metastases. *Neuroradiology* 2003;45:44–49 [CrossRef Medline](#)
- Chiang IC, Kuo Y-T, Lu C-Y, et al. Distinction between high-grade gliomas and solitary metastases using peritumoral 3T magnetic resonance spectroscopy, diffusion, and perfusion imaging. *Neuroradiology* 2004;46:619–27 [CrossRef Medline](#)
- Bulakbasi N, Kocaoglu M, Farzaliyev A, et al. Assessment of diagnostic accuracy of perfusion MR imaging in primary and metastatic solitary malignant brain tumors. *AJNR Am J Neuroradiol* 2005;26:2187–99 [Medline](#)
- Calli C, Kitis O, Yuntun N, et al. Perfusion and diffusion MR imaging in enhancing malignant cerebral tumors. *Eur J Radiology* 2006;58:394–403 [CrossRef Medline](#)
- Fayed N, Dávila J, Medrano J, et al. Malignancy assessment of brain tumours with magnetic resonance spectroscopy and dynamic susceptibility contrast MRI. *Eur J Radiology* 2008;67:427–33 [CrossRef Medline](#)
- Zhang H, Rödiger LA, Zhang G, et al. Differentiation between supratentorial single brain metastases and high grade astrocytic tumors: an evaluation of different DSC MRI measurements. *Neuroradiol J* 2009;22:369–77 [CrossRef Medline](#)
- Huang BY, Kwok L, Castillo M, et al. Association of choline levels and tumor perfusion in brain metastases assessed with proton MR spectroscopy and dynamic susceptibility contrast-enhanced perfusion weighted MRI. *Technol Cancer Res Treat* 2010;9:327–37 [CrossRef Medline](#)
- Hakyemez B, Erdogan C, Gokalp G, et al. Solitary metastases and high-grade gliomas: radiological differentiation by morphometric analysis and perfusion-weighted MRI. *Clin Radiology* 2010;65:15–20 [CrossRef Medline](#)
- Server A, Orheim TED, Graff BA, et al. Diagnostic examination performance by using microvascular leakage, cerebral blood volume, and blood flow derived from 3-T dynamic susceptibility-weighted contrast-enhanced perfusion MR imaging in the differentiation of glioblastoma multiforme and brain metastasis. *Neuroradiology* 2011;53:319–30 [CrossRef Medline](#)
- Mangla R, Kolar B, Zhu T, et al. Percentage signal recovery derived from MR dynamic susceptibility contrast imaging is useful to differentiate common enhancing malignant lesions of the brain. *AJNR Am J Neuroradiol* 2011;32:1004–10 [CrossRef Medline](#)
- Zhang H, Zhang G, Oudkerk M. Brain metastases from different primary carcinomas: an evaluation of DSC MRI measurements. *Neuroradiol J* 2012;25:67–75 [CrossRef Medline](#)
- Tsougos I, Svolos P, Kousi E, et al. Differentiation of glioblastoma multiforme from metastatic brain tumor using proton magnetic resonance spectroscopy, diffusion and perfusion metrics at 3 T. *Cancer Imaging* 2012;12:423–36 [CrossRef Medline](#)
- Tsolaki E, Svolos P, Kousi E, et al. Automated differentiation of glioblastomas from intracranial metastases using 3T MR spectroscopic and perfusion data. *Int J Comput Assist Radiology Surg* 2013;8:751–61 [CrossRef Medline](#)
- Bauer AH, Erly W, Moser FG, et al. Differentiation of solitary brain metastasis from glioblastoma multiforme: a predictive multiparametric approach using combined MR diffusion and perfusion. *Neuroradiology* 2015;57:697–703 [CrossRef Medline](#)
- She D, Xing Z, Cao D. Differentiation of glioblastoma and solitary brain metastasis by gradient of relative cerebral blood volume in the peritumoral brain zone derived from dynamic susceptibility contrast perfusion magnetic resonance imaging. *J Comput Assist Tomogr* 2019;43:13–17 [CrossRef Medline](#)
- Askaneer K, Rydelius A, Engelholm S, et al. Differentiation between glioblastomas and brain metastases and regarding their primary site of malignancy using dynamic susceptibility contrast MRI at 3T. *J Neuroradiol* 2019;46:367–72 [CrossRef Medline](#)
- Chakhoyan A, Raymond C, Chen J, et al. Probabilistic independent component analysis of dynamic susceptibility contrast perfusion MRI in metastatic brain tumors. *Cancer Imaging* 2019;19:14 [CrossRef Medline](#)
- Aslan K, Gunbey HP, Tomak L, et al. Multiparametric MRI in differentiating solitary brain metastasis from high-grade glioma: diagnostic value of the combined use of diffusion-weighted imaging, dynamic susceptibility contrast imaging, and magnetic resonance spectroscopy parameters. *Neurol Neurochir Pol* 2019;53:227–37
- Surendra KL, Patwari S, Agrawal S, et al. Percentage signal intensity recovery: a step ahead of rCBV in DSC MR perfusion imaging for the differentiation of common neoplasms of brain. *Indian J Cancer* 2020;57:36–43 [CrossRef Medline](#)
- Cindil E, Sendur HN, Cerit MN, et al. Validation of combined use of DWI and percentage signal recovery-optimized protocol of DSC-MRI in differentiation of high-grade glioma, metastasis, and lymphoma. *Neuroradiology* 2021;63:331–42 [CrossRef Medline](#)
- Lavrova A, Teunissen WHT, Warnert EAH, et al. Diagnostic accuracy of arterial spin labeling in comparison with dynamic susceptibility contrast-enhanced perfusion for brain tumor surveillance at 3T MRI. *Front Oncol* 2022;12:849657 [CrossRef Medline](#)
- Kamimura K, Nakajo M, Gohara M, et al. Differentiation of heman-glioblastoma from brain metastasis using MR amide proton transfer imaging. *J Neuroimaging* 2022;32:920–29 [CrossRef Medline](#)
- Semmineh NB, Bell LC, Stokes AM, et al. Optimization of acquisition and analysis methods for clinical dynamic susceptibility contrast MRI using a population-based digital reference object. *AJNR Am J Neuroradiol* 2018;39:1981–88 [CrossRef Medline](#)
- Kamimura K, Kamimura Y, Nakano T, et al. Differentiating brain metastasis from glioblastoma by time-dependent diffusion MRI. *Cancer Imaging* 2023;23:75 [CrossRef Medline](#)
- Ahir BK, Engelhard HH, Lakka SS. Tumor development and angiogenesis in adult brain tumor: glioblastoma. *Mol Neurobiol* 2020;57:2461–78 [CrossRef Medline](#)
- Boxerman JL, Quarles CC, Hu LS, et al; Jumpstarting Brain Tumor Drug Development Coalition Imaging Standardization Steering Committee. Consensus recommendations for a dynamic susceptibility contrast MRI protocol for use in high-grade gliomas. *Neuro Oncol* 2020;22:1262–75 [CrossRef Medline](#)
- Bedekar D, Jensen T, Schmainda KM. Standardization of relative cerebral blood volume (rCBV) image maps for ease of both inter- and intrapatient comparisons. *Magn Reson Med* 2010;64:907–13 [CrossRef Medline](#)
- Prah MA, Stufflebeam SM, Paulson ES, et al. Repeatability of standardized and normalized relative CBV in patients with newly

- diagnosed glioblastoma. *AJNR Am J Neuroradiol* 2015;36:1654–61 [CrossRef Medline](#)
36. Schmainda KM, Prah MA, Marques H, et al. Value of dynamic contrast perfusion MRI to predict early response to bevacizumab in newly diagnosed glioblastoma: results from ACRIN 6686 multicenter trial. *Neuro Oncol* 2021;23:314–23 [CrossRef Medline](#)
37. Schmainda KM, Prah MA, Rand SD, et al. Multisite concordance of DSC-MRI analysis for brain tumors: results of a National Cancer Institute Quantitative Imaging Network Collaborative Project. *AJNR Am J Neuroradiol* 2018;39:1008–16 [CrossRef Medline](#)
38. Schmainda KM, Prah MA, Zhang Z, et al. Quantitative Delta T1 (dT1) as a replacement for adjudicated central reader analysis of contrast-enhancing tumor burden: a subanalysis of the American College of Radiology Imaging Network 6677/Radiation Therapy Oncology Group 0625 Multicenter Brain Tumor Trial. *AJNR Am J Neuroradiol* 2019;40:1132–39 [CrossRef Medline](#)
39. Boxerman JL, Schmainda KMM, Weisskoff RMM. Relative cerebral blood volume maps corrected for contrast agent extravasation significantly correlate with glioma tumor grade, whereas uncorrected maps do not. *AJNR Am J Neuroradiol* 2006;27:859–67 [Medline](#)
40. Whitfield BT, Huse JT. Classification of adult-type diffuse gliomas: impact of the World Health Organization 2021 update. *Brain Pathol* 2022;32:e13062. [CrossRef Medline](#)
41. Berghoff AS, Preusser M. Anti-angiogenic therapies in brain metastases. *Memo* 2018;11:14–17
42. Schmainda KM, Prah MA, Hu LS, et al. Moving toward a consensus DSC-MRI protocol: validation of a low-flip angle single-dose option as a reference standard for brain tumors. *AJNR Am J Neuroradiol* 2019;40:626–33 [CrossRef Medline](#)
43. Donahue KM, Krouwer H, Rand SD, et al. Utility of simultaneously acquired gradient-echo and spin-echo cerebral blood volume and morphology maps in brain tumor patients. *Magn Reson Med* 2000;43:845–53 [CrossRef](#)
44. Prah MA, Al-Gizawiy MM, Mueller WM, et al. Spatial discrimination of glioblastoma and treatment effect with histologically-validated perfusion and diffusion magnetic resonance imaging metrics. *J Neurooncol* 2018;136:13–21 [CrossRef Medline](#)
45. Hoxworth JM, Eschbacher JM, Gonzales AC, et al. Performance of standardized relative CBV for quantifying regional histologic tumor burden in recurrent high-grade glioma: comparison against normalized relative CBV using image-localized stereotactic biopsies. *AJNR Am J Neuroradiol* 2020;41:408–15 [CrossRef Medline](#)
46. Iv M, Liu X, Lavezo J, et al. Perfusion MRI-based fractional tumor burden differentiates between tumor and treatment effect in recurrent glioblastomas and informs clinical decision-making. *AJNR Am J Neuroradiol* 2019;40:1649–57 [CrossRef](#)
47. Connelly JM, Prah MA, Santos-Pinheiro F, et al. Magnetic resonance imaging mapping of brain tumor burden: clinical implications for neurosurgical management: case report. *Neurosurgery Open* 2021;2:okab029 [CrossRef Medline](#)
48. Skogen K, Schulz A, Dormagen JB, et al. Diagnostic performance of texture analysis on MRI in grading cerebral gliomas. *Eur J Radiology* 2016;85:824–29 [CrossRef Medline](#)
49. Hu LS, Eschbacher JM, Heiserman JE, et al. Reevaluating the imaging definition of tumor progression: perfusion MRI quantifies recurrent glioblastoma tumor fraction, pseudoprogression, and radiation necrosis to predict survival. *Neuro Oncol* 2012;14:919–30 [CrossRef Medline](#)